Atmospheric Environment 199 (2019) 177–188

Contents lists available at ScienceDirect

Atmospheric Environment

journal homepage: www.elsevier.com/locate/atmosenv

Atmospheric mercury emissions from two pre-calciner cement plants in Southwest China

Xinyu Li[a,b], Zhonggen Li[a,*], Tingting Wu[a], Ji Chen[a], Chengcheng Fu[c], Leiming Zhang[d], Xinbin Feng[a,**], Xuewu Fu[a], Li Tang[a], Zhikang Wang[e], Zhibo Wang[e]

[a] State Key Laboratory of Environmental Geochemistry, Institute of Geochemistry, Chinese Academy of Sciences, Guiyang, 550081, China
[b] University of Chinese Academy of Sciences, Beijing, 100049, China
[c] Guizhou Environmental Monitoring Center, Guiyang, 550081, China
[d] Air Quality Research Division, Science and Technology Branch, Environment and Climate Change Canada, Toronto, Canada
[e] College of Eco-environmental Engineering, Guizhou Minzu University, Guiyang, 550025, China

GRAPHICAL ABSTRACT

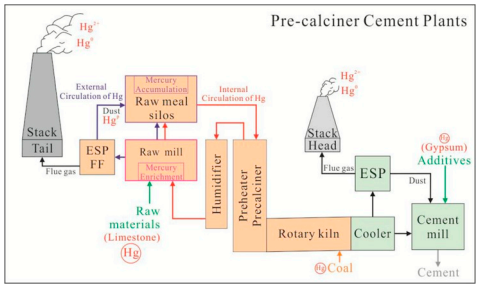

ARTICLE INFO

Keywords:
Atmospheric mercury emissions
Air pollution control
Emission factor
Mercury enrichment
Cement plant

ABSTRACT

China produces the most cement product worldwide, and cement plants (CPs) have been regarded as the largest anthropogenic sources of atmospheric mercury (Hg) emissions in China since 2009. Onsite studies of this source are scarce compare to the huge numbers of CPs in China. Hence, quantifying Hg emissions from more CPs is needed in reducing the large uncertainties existed in the current Hg emission inventories and for assessing subsequent impacts of Hg on human and ecosystem health. In this study, two pre-calciner CPs in Guizhou province of Southwest China were selected for quantifying the emission factor and mass balance of Hg. Results showed that Hg emission levels in the two CPs were obviously different due to the differences in Hg input and circulation in the production system. In cement plant #1 (CP #1), the input and output of Hg reached a dynamic equilibrium condition, the emission factor was 76.1 mg $Hg{\cdot}t^{-1}$ clinker, and Hg concentration in the stack flue gas was in the range of 14.46–16.64 μg m^{-3}. In cement plant #2 (CP #2), Hg was in an enriching status because it was a new plant with operation of several months and most input Hg was retained inside the production system, hence with a much lower emission factor of 1.8 mg $Hg{\cdot}t^{-1}$ clinker and Hg concentration of 0.15–0.49 μg m^{-3} in the stack gas. Kiln tail stack was the main output pathway of Hg in the clinker production process. With removal efficiency of 73.06% and 99.95% at kiln tail by ESP in CP #1 and humidifier + ESP-FF in CP #2, respectively, Hg emitted into the atmosphere was mainly in the forms of gaseous oxidized mercury (Hg^{2+}) and gaseous elemental mercury (Hg^0). Besides, the operation mode (on or off) of raw mill had great impact on the concentration and speciation of Hg in flue gas and flue gas temperature at kiln tail. In the clinker production system,

* Corresponding author.
** Corresponding author.
E-mail addresses: lizhonggen@mail.gyig.ac.cn (Z. Li), fengxinbin@mail.gyig.ac.cn (X. Feng).

https://doi.org/10.1016/j.atmosenv.2018.11.011
Received 22 April 2018; Received in revised form 23 September 2018; Accepted 5 November 2018
Available online 10 November 2018

limestone is the main source of Hg input (41.4–56.4%), followed by the fueled coal (15.3–32.5%). While, in the clinker to cement production process, the additives (mainly gypsum from coal-fired power plants, 83.2–94.4%) was the main source of Hg in the cement because Hg concentration in the clinker was very low.

1. Introduction

Mercury (Hg) is one of the most toxic heavy metals in the environment and its pollution has become one of the focuses of environmental concerns worldwide because of its long-range transport in air and bio-accumulation in food chain (Chang et al., 2000; Schroeder and Munthe, 1998; Nriagu and Pacyna, 1988; Sheu and Mason, 2001; Landis et al., 2004; Lindberg et al., 2007; Zhang and Jaeglé, 2013). Since the Minamata disease happened in 1953 in Japan, Hg has been regarded as a highly dangerous global pollutant by United Nations Environment Programme and World Health Organization (UNEP, 2013; WHO, 1991). Hg in the atmosphere exists as three operationally defined forms: gaseous elemental mercury (Hg^0), gaseous oxide mercury (Hg^{2+}) and particulate-bound mercury (Hg^p). Hg can be emitted from natural and anthropogenic sources (Zhang et al., 2016), with the former mainly include marine/soil surface emissions, biomass combustion, volcanic eruption, etc. (Nriagu, 1989; Pirrone et al., 2010), and the latter include fossil fuel combustion, nonferrous metal smelting, cement production, waste incineration, etc. (Nriagu and Pacyna, 1988; Lee et al., 2014). Atmospheric Hg, once deposited to aquatic systems through dry and wet deposition, can be methylated into methylmercury, a form that can be accumulated in fish and then consumed by human being through the food chain (Renzoni et al., 1998). In the past two centuries, with the intensified human activities, the quantities of Hg emitted into atmosphere from anthropogenic sources has increased substantially (Streets et al., 2011, 2017; Wu et al., 2006; Tian et al., 2010) and has caused adverse effects on the ecological environment (UNEP, 2013).

Due to the economic development and increasing energy demand, the developing countries have become the most important emission sources of Hg to the atmosphere (UNEP, 2013; Pham et al., 2015) and the Hg released in the northern hemisphere is much higher than that in the southern hemisphere (Streets et al., 2017; Travnikov, 2005). Asia has been recognized as a region with the highest anthropogenic emissions of Hg in the world during the past three decades (Streets et al., 2011; UNEP, 2002, 2013; Pacyna et al., 2002, 2006, 2010), and China is the largest one in this region with emissions of 500–800 t y^{-1}, accounting for about 1/4–1/3 of the total globally (Wu et al., 2006, 2016; Pacyna et al., 2010). Earlier assessments suggested that artisanal and small scale gold mining and fossil fuel combustion were the largest two anthropogenic Hg emission sources in the world (UNEP, 2013; Pacyna et al., 2006), but Hg emissions from the other sources, such as nonferrous smelting (Pb/Zn/Cu) and cement production, have been increasing in recent years (Wu et al., 2016). Hg emissions from anthropogenic sources in China were estimated to be at 538 t in 2010, of which coal combustion (48%, coal-fired power plants accounted 19%, industrial coal combustion accounted 22% and other coal combustion accounted 7%), cement production (18%) and zinc smelting (12%) were the top three contributors (Zhang et al., 2015). The accumulated Hg emissions during 1978–2014 from anthropogenic sources in China were estimated to be at 13,294 t Hg, and cement production has been regarded as the largest anthropogenic source since 2009, its emission showed continuous increase trend even the national total Hg emission from all anthropogenic sources has been reduced since 2012 (Wu at el., 2016).

Various cement types have been invented, such as common, slag, pozzolanic, fly ash and composite cements (Xiao and Li, 2006; Zhou and Peng, 2005). The common cement, also known as Portland cement, is the most commonly used cement. It is made of raw material like limestone, clay, shale, iron ore, etc. Comminuted raw materials are sintered at high temperature (up to 1500 °C) to produce clinker, which is then mixed with some additives like gypsum and fly ash to produce cement. For some special cements, bauxite, kaolin, quartz and volcanic ash should also be added in the production process from clinker to cement (Wang et al., 2007; Wu, 1999). However, Hg concentrations in raw materials varied greatly, e.g., from 0.004 to 2.753 (average 0.043) mg·kg^{-1} in limestone (Yang, 2014) and from 0.01 to 0.5 mg kg^{-1} in coal used as fuel during the clinker production (Tang, 2004). In addition, Hg in the raw materials will evaporate at high temperature of calcination, form a mixture of Hg^p, Hg^0 and Hg^{2+} when the flue gas is cooling down, then interact with the raw materials, and finally discharge into the atmosphere with flue gas (Sikkema et al., 2011; Galbreath and Zygarlicke, 2000).

China is the largest cement producer in the world and the cement production reached to 2.4×10^9 t in 2016, accounting for more than half of the world's total production (National Bureau of Statistic of China, 2017). With the development of the cement manufacturing techniques, the cement production process used in China has changed significantly since 2000. The proportion of the pre-calciner process increased from 10% in 2000 to 91% in 2012 (Hua et al., 2016), noting that the shaft process dominated before 2000. Compared with the traditional shaft kiln, the pre-calciner process can operate continuously to improve the production efficiency and reuse the energy from the rotary kiln to pre-heat and pre-calcine the raw material, hence save the energy. Besides, it also can produce higher quality cement and have better emission control. The pre-calciner process mainly includes the following four steps: raw material broken and homogenization, preheating and decomposition, clinker production, and milling and packing (Zhou and Peng, 2005; Ma, 2007). The total number of pre-calciner cement production lines in China reached to about 1800 in 2016, but to date only less than 20 of these production lines have been investigated for Hg emissions (Wang, 2017; Miao et al., 2015; Li, 2011; Yang, 2014; Zhang, 2007; Zhang et al., 2017).

Considering the different raw materials, associated Hg contents and techniques of air pollution control devices (APCDs) used in different cement plants (CPs), it's imperative to conduct more on-site field measurements in representative CPs and production procedures to quantify Hg emissions from this industry and reveal the associated impacting factors controlling Hg emissions in China. In this study, Hg emissions from two CPs with pre-calciner process in Guizhou province, Southwest China, were investigated by measuring concentration and speciation of Hg in flue gases. Hg concentrations in solid samples during the cement production processes were also sampled and analyzed. The concentrations of speciated Hg in the flue gas were compared before and after APCDs, and the mass balance of Hg and mercury emission factors (MEF) from two tested CPs were calculated. Knowledge generated from this study is useful for reducing the uncertainties of the estimated Hg emissions and for formulating solutions to reduce Hg emissions from this source sector.

2. Methodology

2.1. Selected cement plants

Guizhou province, located in southwest China, reserves large amounts of limestone and coal resources and is one of the major provinces for cement production in China. The cement output of Guizhou Province increased from 15.6×10^6 t in 2005 to 107.5×10^6 t in 2016, accounting for about 4.5% of the national production in 2016 (Bureau of statistics of Guizhou Province, 2017). Two CPs in Guizhou Province

were selected for Hg study with CP #1 located in the eastern part of Guizhou province and 22 km northwest of Wanshan Hg mine, the largest mercury mine in China, and CP #2 located in the central part of Guizhou province where there is no Hg and other heavy metal minerals around.

At the time the present experiments were carried out (August and December 2015 for CP #1 and CP #2, respectively), the cement production lines had been operated for 1.5 and 0.5 years, respectively. Limestone used in the two CPs was produced locally (within 1–2 km) since Guizhou is mainly Karst landform. Coal used in CP #1 was produced from central China (Henan and Shaanxi provinces) and that in CP #2 from western part of Guizhou. Details about production capacities and APCDs in the two CPs are shown in Table 1. APCDs comprised of ESP at kiln head and SNCR + ESP (CP #1) or SNCR + ESP-FF (CP #2) at kiln tail, SNCR was used to control the NOx emissions by spaying urea at high temperature (800–900 °C) zone and thought to have no effect on Hg reduction. In the clinker production process, raw materials (limestone, clay, sandstone, Fe material, coal gangue, etc.) are first processed using grinder and homogenizing device, and then the comminuted and mixed raw materials are ground further in a raw mill to produce raw meal. After passing through the preheater and pre-calciner successively, raw meal is heated further by burning coal in a rotary kiln to produce clinker. Finally, in the production process of cement, clinker is blended with a certain proportion of additional materials (limestone, gypsum and fly ash from the coal-fired power plants) in the cement mill to produce various types of cements.

Atmospheric Hg emissions from flue gas were tested for kiln tail and head, but not for coal mill considering a minor proportion (< 9%) of Hg discharged from the later pathway (Wang et al., 2014). The kiln tail is one end of the rotary kiln, where the pre-calcined raw meal enters into the rotary kiln and the flue gas leaves. The kiln head is another end of the rotary kiln, where clinker is produced and cooled, and coal powder is injected into the rotary kiln to heat the raw meal. During the operation period of CPs, the raw mill will be closed for a period of time according to the situation of production line. When the raw mill is operated (on mode), flue gas flows through the raw mill first before entering into APCDs and finally emitting from the stack at the kiln tail. If the raw mill is shut down (off mode), flue gas will not pass through the raw mill but will enter APCDs directly (Fig. 1, Wang et al., 2014). The sampling locations and the sample types in this study are shown in Table 1 and Fig. 1. The sampling locations for solid samples and flue gas at the outlet of dust collector at kiln head and kiln tail were the same for both CPs, expect the site for flue gas before dust collector at kiln tail, i.e. it was ESP inlet in CP #1 and humidifier inlet in CP #2, respectively. The humidifier was used to adjudge the flue gas humidity and reduce the flue gas temperature. Water was spayed into humidifier and flue gas temperature dropped from 310 °C at the humidifier inlet to about 130 °C at the ESP-FF inlet, this will enhance the removal of soluble Hg (such as gaseous divalent Hg) from the flue gas and more gaseous Hg will adsorb onto the particulate matters.

2.2. Sampling methods

Flue gas at the kiln head and tail was sampled using the Ontario Hydro Method (OHM, Model XC-572, Apex Instruments, USA) according to ASTM Method 6784-02 (2008) (Fig. S1), which can separate the three operational defined Hg species, i.e. Hg^0, Hg^{2+} and Hg^p. Hg^p is first collected on the glass fiber filter, and an additional glass cyclone is used before the glass fiber filter when the flue gas contained too much particulate matters (mainly before ESP/FF). Three impingers containing KCl solution (1 mol L^{-1}) are then used to capture Hg^{2+}. One impinger with H_2O_2 + HNO_3 (10% v/v + 5% v/v) and three impingers with H_2SO_4 + $KMnO_4$ solution (10% v/v + 4% m/v) jointly collect Hg^0 through oxidation and absorption processes. In the end, an impinger with silica gel is used to remove moisture in flue gas. All impingers were stored in an ice bath to ensure a low temperature condition and absorb Hg completely. Both the probe and the filters were heated to at least 120 °C to avoid the water condensation and Hg adsorption on the tubing walls. Each flue gas sample lasted for 1–1.5 h with a flue gas volume of about 0.5–1.3 m^3. In the laboratory, Hg in each impinger was recovered by $SnCl_2$ and measured at least twice by Cold Vapor Atomic Absorption Spectrophotometry (CVAAS, F732S, Shanghai Huaguang Instrument Corp), which has a detection limit of 0.05 μg L^{-1}.

Solid materials, including different raw materials, intermediate products, clinker and additives, were collected during the flue gas sampling. Three to six samples (each about 1 kg) of each kind of solid samples, reflecting different time periods, were gathered. The solid samples were dried at 40 °C, then homogenized and grounded to less than 150 μm. The US EPA Method 7473 was adopted to determine Hg concentrations in solid samples, which heat solid samples at 800 °C and measure the released Hg^0 by CVAAS (Lumex RA915+, Russia) with a detection limit of 0.1 μg kg^{-1}. Each solid sample was determined at least three times to obtain a mean value.

2.3. Quality assurance and quality control

All sampling lines (quartz glass and teflon tubings), impingers and bottles used in the flue gas sampling were soaked into a 20% nitric acid liquid overnight in the laboratory and washed with deionized water before sampling. The systematic blank of sampling the ambient air in the laboratory was determined before each field experiment, which was found to be 0.05 μg m^{-3}. Hg concentrations of reagents used in the experiments were below the detection limit, except H_2SO_4 (ca. 1.2 ng Hg·mL^{-1} concentrated), which compromised about 80% of the systematic blank. Certified reference materials stand for limestone, coal, fly ash and soil (JDo-1, NIST 1632d, NIST 1633c, GBW 08401, GBW 07405) were used to guarantee the analytical quality, and the recovery of Hg was found to be in the range of 98–105%.

3. Results and discussion

3.1. Total and speciation of Hg in the flue gas

The detailed information of Hg in flue gas of the tested CPs is illustrated in Tables 2 and 3. The operational mode of raw mill had obvious influence on flue gas temperature and Hg concentration in the flue gas at kiln tail. For example, sampling runs #3 and #4 at the kiln tail of CP #1, when the raw mill was in off mode, had much higher flue gas temperatures and Hg concentrations than those of sampling runs #1 and #2, when the raw mill was in on mode. The temperature increased

Table 1
The process of studied CPs and the APCDs and flue gas sampling locations.

Cement plant	Process types	Production capacity (t clinker·day^{-1} $line^{-1}$)	APCDs[a]		Flue gas sampling locations
			kiln head	kiln tail	
CP #1	Preheater/Pre-calciner	4500	ESP	SNCR + ESP	stack of the kiln head, inlet of ESP and stack of the kiln tail
CP #2	Preheater/Pre-calciner	5000	ESP	SNCR + ESP-FF	stack of the kiln head, inlet of humidifier and stack of the kiln tail

[a] , ESP: Electrostatic precipitator; SNCR: Selective non-catalytic reduction; FF: Fabric filter.

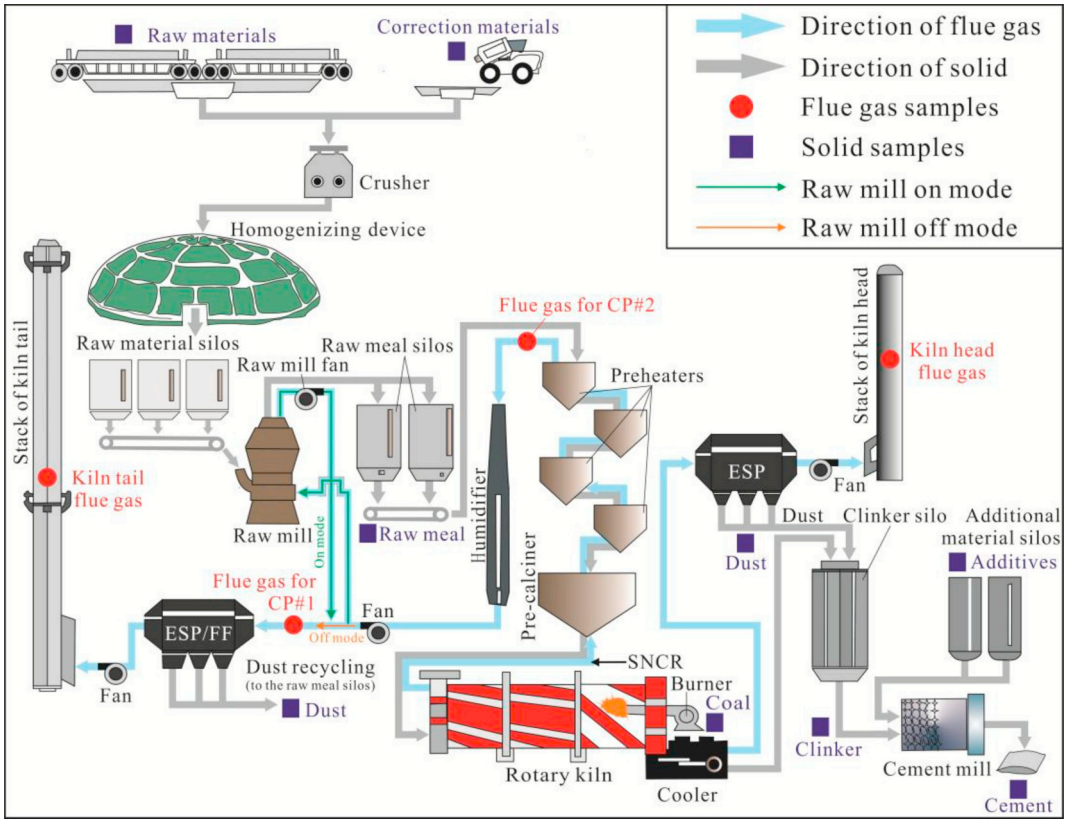

Fig. 1. Schematic diagram of the preheater/pre-calciner cement manufacturing facility and the sampling points.

from 85 - 88 °C in on mode to 125–134 °C in off mode, and the total concentration of Hg (THg) in flue gas increased from 19.2 μg m^{-3} to 191.7 μg m^{-3} at ESP inlet, and from 8.08 μg m^{-3} to 40.0 μg m^{-3} at the stack. The role of raw mill on flue gas temperature and Hg concentration was also found in CPs in Slovenia and other countries (Mlakar et al., 2010; Senior et al., 2010). In the on mode situation, THg in stack flue gas of kiln head and tail was 16.6 μg m^{-3} and 8.08 μg m^{-3} for CP #1 and 0.15 μg m^{-3} and 0.49 μg m^{-3} for CP #2, respectively. The on mode and off mode situation accounted for approximately 80% and 20% of production time in CP #1, respectively, these information was used for calculating the weighted average values (WAV) to represent the final Hg concentration at the kiln tail of CP #1. However, flue gas samples were only collected in raw mill on mode situation in CP #2, so the arithmetic mean (AM) was used to represent the final Hg concentration at the kiln tail of CP #2. Although the Hg emissions from kiln tail of CP #1 increased in a certain extent after weighted calculation (from 8.08 μg m^{-3} to 14.5 μg m^{-3}), THg of the stack emissions of both the two CPs was lower than the standard limit for cement industry in China (50 μg m^{-3}, GB 4915-2013) and the United States (41 μg m^{-3}, Discharge standards of harmful air pollutant from Portland cement kiln), as shown in Figs. 2 and 3.

Speciation of Hg in the flue gas of the two CPs was quite different (Figs. 2 and 3). In the on mode of CP #1, Hg^p was 9.82 μg m^{-3} (accounted for 51.2% of THg) before ESP at the kiln tail and was negligible (0.02 μg m^{-3}, 0.22%) after ESP. And Hg^{2+} declined but that of Hg^0 increased across the ESP, implying that the reduction of Hg^{2+} to Hg^0 occurred at ESP in the on mode. While, in the off mode, when the flue gas was not circulated into raw mill, all speciated Hg sharply increased at the inlet and outlet of ESP compared to the on mode, meanwhile, both Hg^{2+} and Hg^0 decreased significantly across the ESP, that might be related to the oxidation of Hg^0 to Hg^{2+} embodied in the decrease of Hg^0, and the removal of Hg^{2+} by adsorbing on the particulate matters embodied in the decrease of total gaseous mercury (Hg^0+Hg^{2+}). However, the concentrations of Hg^p, Hg^{2+} and Hg^0 fluctuated greatly between the two sampling runs in the off mode, implying the large variation of Hg in the flue gas in off mode and more onsite sampling are needed in accurately quantify the emission levels. Nevertheless, the operation of raw mill had positive effects on reducing the particulate Hg (Hg^p) and gaseous Hg (Hg^{2+} and Hg^0) emission from kiln tail in CPs. Hg emitted from the stack of kiln tail in CP #1 was mainly composed of Hg^0 (64.6%) and Hg^{2+} (35.2%) after the weighted calculation. At the stack of kiln head in CP #1, nearly all THg was in the form of Hg^{2+} (99.3%) and only a few percent in the form of Hg^0 and Hg^p, that might be due to some compositions in the raw material, such as silicon (sandstone) and Fe material, that favors the oxidation of Hg (He et al., 2016). After APCDs, THg concentration was similar between the kiln tail (14.5 μg m^{-3}) and the kiln head (16.6 μg m^{-3}). In CP #2, Hg^p was the dominate portion (97.0%) of THg in flue gas before the humidifier at kiln tail, and THg (902 μg m^{-3}) was far more than that of CP #1 before ESP at kiln tail (53.7 μg m^{-3}) (Tables 2 and 3). In comparison, THg declined to 0.49 μg m^{-3} after the combined control by humidifier and ESP-FF, with share and concentration of Hg^{2+} (78.1%, 0.37 μg m^{-3}), Hg^p (17.1%, 0.10 μg m^{-3}) and Hg^0 (4.7%, 0.02 μg m^{-3}). This result may be caused by three reasons as follow: 1) the tremendous temperature drops (from 309 °C to 80 °C) across the humidifier facilitated more gaseous Hg (Hg^{2+} and Hg^0) adsorbed on particulate matters; 2) a portion of Hg in the flue gas at the kiln tail was absorbed by raw meal at raw mill in on mode, which enriched and circulated Hg in the clinker production process; 3) ESP-FF had higher removal efficiency than that of ESP. Besides, THg in stack flue gas at kiln head of CP #2 was very low at 0.1–0.2 μg m^{-3}, nearly equally distributed between Hg^{2+} (42.4%) and Hg^0 (56.4%).

Compared with the other studies worldwide (Table S1 and Fig. S2), out results are within the range found for THg in stack emissions, which ranged from 0 to 67 μg m^{-3} with most values being below 30 μg m^{-3}. Generally, Hg in stack flue gas from CPs comprised of gaseous Hg (Hg^0 and Hg^{2+}) in majority, with a small proportion of Hg^p, because of almost all particulate matter in the flue gas was removed by the high

Table 2
Total and speciated Hg in the flue gas and associated parameters of the flue gas of CP #1.

Sampling point	Test Number	Date	Time period	Sample volume (m^3)	Flue gas temperature (°C)	Moisture content (%)	Hg^p ($\mu g \cdot m^{-3}$)	Hg^{2+} ($\mu g \cdot m^{-3}$)	Hg^0 ($\mu g \cdot m^{-3}$)	THg ($\mu g \cdot m^{-3}$)	Proportion of speciated Hg (%)		
											Hg^p	Hg^{2+}	Hg^0
Before ESP of kiln tail	#1[a]	2015-08-04	15:25–16:42	0.77	85	8.59	10.19	7.96	1.92	20.1	50.8	39.7	9.6
	#2[a]	2015-08-04	17:25–18:40	0.86	84	7.54	9.46	6.67	2.22	18.4	51.5	36.3	12.1
	#3[b]	2015-08-05	07:36–09:20	0.64	137	9.78	141.2	26.4	8.93	176.5	80.0	15.0	5.1
	#4[b]	2015-08-05	12:08–13:24	0.57	131	6.34	98.76	94.0	14.1	206.8	47.8	45.5	6.8
	Average (on mode)[a]			0.82	85	8.07	9.82	7.32	2.07	19.2	51.2	38.0	10.9
	Average (off mode)[b]			0.61	134	8.06	120.0	60.2	11.5	191.7	63.9	30.2	5.9
	Weighted average[c]			0.77	94	8.06	31.86	17.9	3.96	53.7	53.7	36.5	9.9
Stack of kiln tail	#1[a]	2015-08-04	15:25–16:40	1.10	89	9.64	0.02	2.79	6.20	9.01	0.2	31.0	68.8
	#2[a]	2015-08-04	17:40–18:55	1.01	86	8.07	0.02	1.70	5.43	7.14	0.2	23.7	76.0
	#3[b]	2015-08-05	08:03–09:27	1.21	126	7.99	0.01	51.7	6.41	58.1	0.0	89.0	11.0
	#4[b]	2015-08-05	09:56–11:22	1.23	123	5.85	0.03	9.61	12.3	21.9	0.1	43.9	56.0
	Average (on mode)[a]			1.06	88	8.86	0.02	2.24	5.81	8.08	0.2	27.4	72.4
	Average (off mode)[b]			1.22	125	6.92	0.02	30.7	9.34	40.0	0.1	66.4	33.5
	Weighted average[c]			1.09	95	8.47	0.02	7.93	6.52	14.5	0.2	35.2	64.6
Stack of kiln head	#1	2015-08-06	09:11–10:27	1.22	98	1.03	0.01	18.3	0.64	18.9	0.0	96.6	3.4
	#2	2015-08-06	10:50–12:05	1.21	97	0.00	0.02	15.6	0.14	15.8	0.1	98.9	0.9
	#3	2015-08-06	15:05–16:20	1.23	97	0.98	0.01	15.1	0.10	15.2	0.1	99.3	0.6
	Range			1.21–1.23	97–98	0.00–1.03	0.01–0.02	15.1–18.3	0.10–0.64	15.2–18.9	0.0–0.1	96.6–99.3	0.6–3.4
	Mean ± SD			1.22 ± 0.01	97 ± 1	0.67 ± 0.58	0.01 ± 0.01	16.3 ± 1.71	0.29 ± 0.30	16.6 ± 2.01	0.1 ± 0.0	98.3 ± 1.5	1.7 ± 1.5

[a] On mode.
[b] Off mode.
[c] Weighted average, with on mode accounted for 80% of the production time, off mode accounted for the rest 20% time.

Table 3
Total and speciated Hg in the flue gas and associated parameters of the flue gas of CP #2.

Sampling point	Test number	Date	Time period	Sample volume (m^3)	Flue gas temperature (°C)	Moisture content (%)	Hg^p ($\mu g \cdot m^{-3}$)	Hg^{2+} ($\mu g \cdot m^{-3}$)	Hg^0 ($\mu g \cdot m^{-3}$)	THg ($\mu g \cdot m^{-3}$)	Proportion of speciated Hg (%)		
											Hg^p	Hg^{2+}	Hg^0
Before the humidifier of kiln tail	#1	2015-12-17	11:27–14:36	0.68	308	4.86	960	13.2	8.91	982	97.8	1.4	0.9
	#2	2015-12-17	15:00–16:03	0.55	309	4.88	791	19.8	11.1	821	96.2	2.4	1.4
	Mean ± SD			0.62 ± 0.09	309 ± 1	4.87 ± 0.01	875 ± 120	16.5 ± 4.63	10.0 ± 1.55	902 ± 114	97.0 ± 1.1	1.9 ± 0.8	1.1 ± 0.3
Stack of kiln tail	#1	2015-12-17	11:00–12:32	1.36	79	4.48	0.17	0.40	0.03	0.60	28.9	66.8	4.3
	#2	2015-12-17	12:38–14:08	1.24	80	6.20	0.02	0.35	0.02	0.39	5.4	89.4	5.2
	Range			1.24–1.36	79–80	4.48–6.20	0.02–0.17	0.35–0.40	0.02–0.03	0.39–0.60	5.4–28.9	66.8–89.4	4.3–5.2
	Mean ± SD			1.30 ± 0.09	80 ± 1	5.34 ± 1.22	0.10 ± 0.11	0.37 ± 0.04	0.02 ± 0.00	0.49 ± 0.15	17.1 ± 16.6	78.1 ± 16.0	4.8 ± 0.6
Stack of kiln head	#1	2015-12-15	15:48–17:01	1.16	77	0.45	0.00	0.13	0.08	0.21	0.8	60.4	38.8
	#2	2015-12-16	10:10–11:25	1.15	75	0.42	0.00	0.04	0.08	0.13	1.3	34.2	64.4
	#3	2015-12-16	11:45–13:15	1.32	73	0.34	0.00	0.04	0.07	0.11	1.5	32.7	65.9
	Range			1.15–1.32	73–77	0.34–0.45	0.00–0.00	0.04–0.13	0.07–0.08	0.11–0.21	0.8–1.5	32.7–60.4	38.8–65.9
	Mean ± SD			1.21 ± 0.10	75 ± 2	0.40 ± 0.05	0.00 ± 0.00	0.07 ± 0.05	0.08 ± 0.01	0.15 ± 0.06	1.2 ± 0.4	42.4 ± 15.6	56.4 ± 15.2

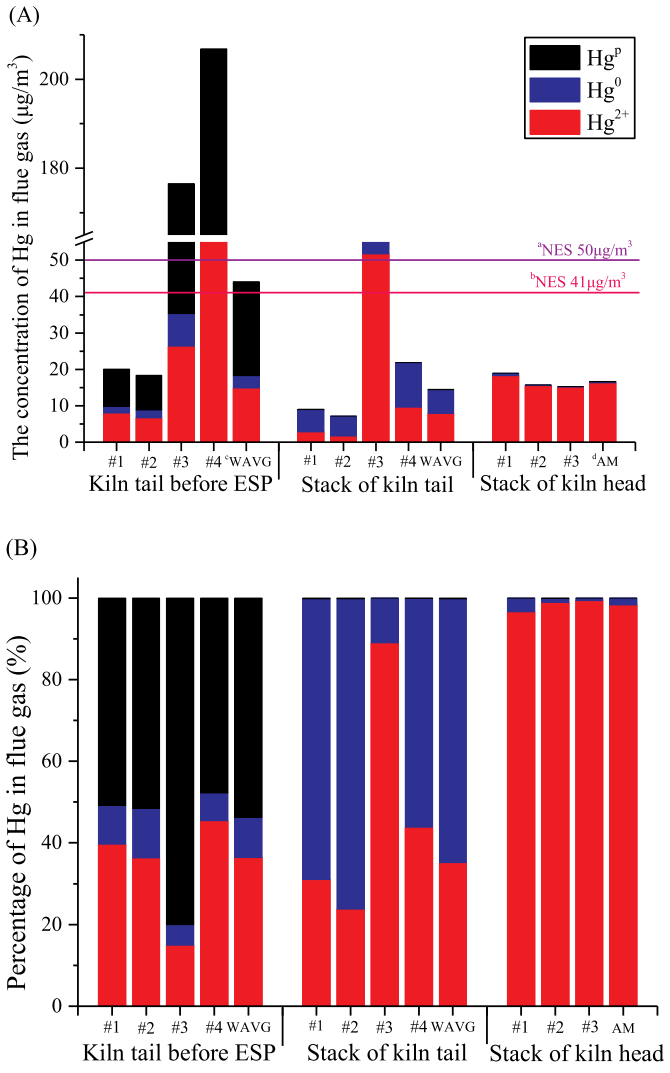

Fig. 2. The speciation of Hg (A) and percentage of different Hg species (B) in flue gas of CP #1.
a, National emission standard for flue gas of cement industry in China.
b, National emission standard for flue gas of cement industry in USA.
c, WAVG: Weighted average.
d, AM: Arithmetic mean.

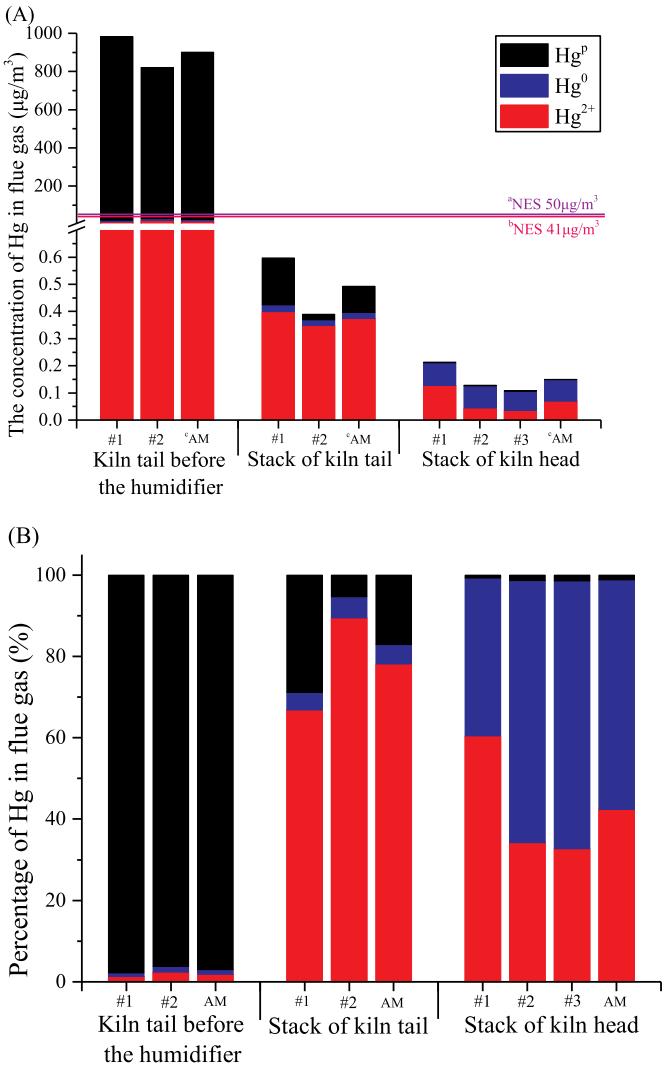

Fig. 3. The speciation of Hg (A) and percentage of different Hg species (B) in flue gas of CP #2.
a, National emission standard for flue gas of cement industry in China.
b, National emission standard for flue gas of cement industry in USA.
c, AM: Arithmetic mean.

efficiency dust collector, ESP or ESP-FF. The concentration of Hg^{2+} and Hg^0 were various in different CPs, such as CPs like CP #1 ($Hg^{2+} < Hg^0$) long other CPs reported by Zhang (2007) and Won and Lee (2012) or CPs like CP #2 ($Hg^{2+} > Hg^0$) and other CPs reported by Mlakar et al. (2010) and Wang et al. (2014). The proportion of them was related to many factors including composition of different kind of raw materials and flue gas, processing temperature, APCDs and so on.

The removal efficiency of speciated Hg in the flue gas at the kiln tail by APCDs in CP #1 and CP #2 is shown in Table 4. A removal efficiency of 73.06% and 99.95% was achieved for THg in CP #1 and CP #2, respectively. Almost all particulate Hg (99.94–99.99%) were captured by APCDs in the two CPs. The removal efficiencies of Hg^{2+} (97.73%) and Hg^0 (99.77%) in CP #2 were substantially higher than those (55.7% and −64.79%) in CP #1. The negative removal efficiency of Hg^0 in CP #1 indicates the reduction of Hg^{2+} into Hg^0 in the ESP. The removal efficiency of Hg in flue gas by APCDs in the two CPs is comparable to recent reports (56–89%) in China (Li, 2011; Miao et al., 2015), but is much higher than those (27–44%) reported for CPs in South Korea (Won and Lee, 2012; Table S1).

3.2. Hg in solid samples and Hg mass balance

Hg contents and material flow of the input material, intermediate and output products in the two CPs are determined and shown in Tables 5 and 6 and Figs. 4 and 5. Although Hg in limestone (7–34 μg kg^{-1}) was lower than that in fueled coal (44–79 μg kg^{-1}), limestone accounted for 41–56% of Hg input in the clinker production system because of its large daily demand. Coal contributed 15–32% of Hg input and the rest of the materials (sandstone, shale, gangue, iron material, etc.) contributed the remaining ca. 30%. These numbers are similar to those found in existing studies, which showed that raw material is the top Hg input followed by fuel in cement kiln (Wang et al., 2014; Mlakar et al.,

Table 4
Removal efficiency of Hg in flue gas by the APCDs installed at kiln tail of tested CPs.

Cement plant	APCDs	Hg^P (%)	Hg^{2+} (%)	Hg^0 (%)	THg (%)
CP #1	ESP	99.94	55.69	−64.79	73.06
CP #2	Humidifier + ESP-FF	99.99	97.73	99.77	99.95

Table 5
Hg mass balance in the clinker production system of CP #1.

Hg input/output and emission factors		Material	Hg concentration (Mean ± SD, μg·kg^{-1})	Material input or output (t·d^{-1})	Hg input or output (g·d^{-1})	Hg input or output percentage (%)
Hg input	Raw material	Limestone	34 ± 22 (n = 5)	5405	182	56.4
		Sandstone	32 ± 3 (n = 3)	432	14	4.3
		Shale	16 ± 14 (n = 3)	431	7	2.1
		Coal gangue	233 ± 183 (n = 2)	103	24	7.5
		Iron-rich materials	191 ± 8 (n = 3)	244	47	14.5
	Fuel	Coal	79 ± 66 (n = 2)	623	49	15.3
	Total				323	100
Intermediate products	Raw meal		272 ± 24 (n = 6)	6784	1845	
	Particulate matter at the kiln head		16 ± 26 (n = 4)	94	1.5	
	Particulate matter at the of kiln tail		3029 ± 493 (n = 6)	138	417	
Hg output	Stack flue gas at the kiln head		16.64[a]	801[b]	133	40.9
	Stack flue gas at the kiln tail		14.46[a]	1310[b]	189	58.1
	Clinker		0.8 ± 0.3 (n = 3)	4241	3	1.0
	Total				326	100
Hg output/input (%)			101			
Hg emission factor (mg Hg·t^{-1} clinker)	Excluded coal		64.5			
	Included coal		76.1 (44.7 from the kiln tail and 31.4 from the kiln head)			
Enrichment factor			5.9			

[a] Unit of Hg concentration in flue gas: μg·m^{-3}.
[b] Unit of flue gas volume: 10^4 m^3 d^{-1}.

Table 6
Hg mass balance in the clinker production system of CP #2. (Note: a line in Table 6 is missing, there always have three lines in a table, but this table just have two)

Hg input/output and emission factors		Material	Hg concentration (Mean ± SD, μg·kg^{-1})	Material input or output (t·d^{-1})	Hg input or output (g·d^{-1})	Hg input or output percentage (%)
Hg input	Raw material	Limestone	6.5 ± 2.1 (n = 5)	6235	41	41.4
		Shale	54 ± 11 (n = 5)	432	23	23.8
		Iron-rich materials	10 ± 4.2 (n = 5)	219	2	2.2
	Fuel	Coal	44 ± 7.8 (n = 5)	723	32	32.5
	Total				98	100
Intermediate products	Raw meal		1313 ± 245 (n = 5)	7723	10140	
	Particulate matter at the kiln head		0.2 ± 0.1 (n = 5)	134	0.03	
	Particulate matter at the of kiln tail		1651 ± 140 (n = 5)	185	305	
Hg output	Stack flue gas at the kiln head		0.15 ± 0.06 (n = 3)[a]	1098[b]	2	11.2
	Stack flue gas at the kiln tail		0.49 ± 0.15 (n = 2)[a]	1486[b]	7	49.6
	Clinker		1.2 ± 0.8 (n = 5)	5025	6	39.2
	Total				15	100
Hg output/input (%)			15			
Hg emission factor (mg Hg·t^{-1} clinker)	Included coal		1.8 (1.5 from the kiln tail and 0.3 from the kiln head)			
Enrichment factor			104			

[a] Unit of Hg concentration in flue gas: μg·m^{-3}.
[b] Unit of flue gas volume: 10^4 m^3 d^{-1}.

2010; Wu et al., 2016). The Hg input in clinker production of CP #1 and CP #2 were 323 g d^{-1} and 98 g d^{-1}, respectively (Tables 5 and 6 and Figs. 4 and 5).

The total Hg output in the clinker production process was 326 g d^{-1} in CP #1, in which 58.1% was from the kiln tail stack flue gas, 40.9% from the kiln head stack flue gas and about 1% from the clinker. In CP #2, the Hg output in the clinker production process was only 15 g d^{-1}, in which 49.6% from the kiln tail stack flue gas, 39.2% from the clinker and 11.2% from the kiln head stack flue gas. Therefore, the kiln tail was the most important pathway for atmospheric Hg emission. Compared with various raw and auxiliary materials (7–233 μg kg^{-1}), as well as the raw meal (272–1313 μg kg^{-1}), Hg concentration in the clinker (0.8–1.2 μg kg^{-1}) was very low, indicating that almost all Hg in raw materials is evaporated into the flue gas during the high temperature production process. The daily release of Hg (output) in CP #1 through stack gas along with clinker was basically the same as the total Hg input

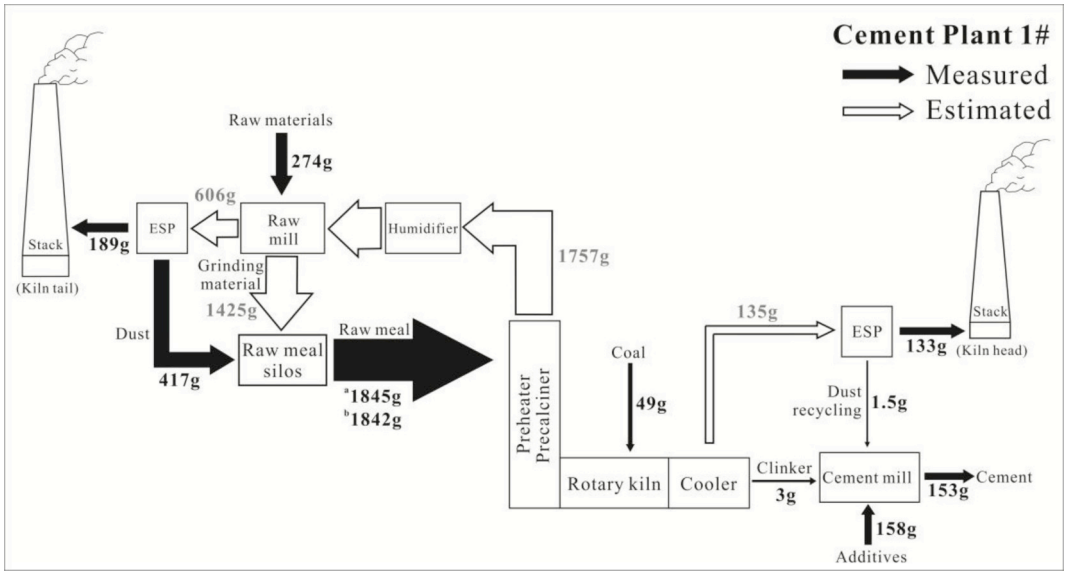

Fig. 4. The mass flow of Hg in CP #1.
The above values are based on 1 day.
a, Test value in the first day; b, Test value in the second day.

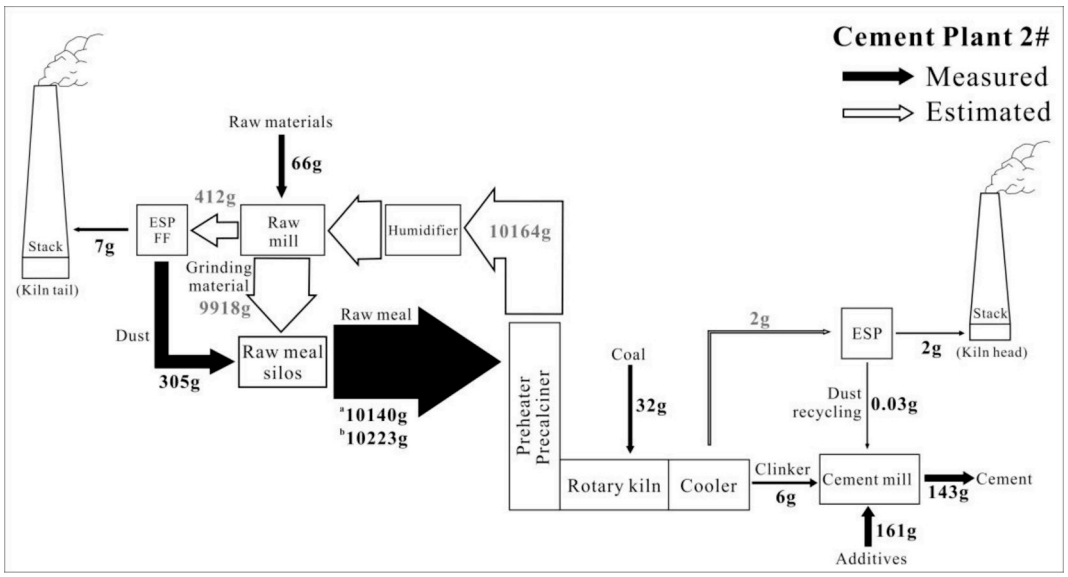

Fig. 5. The mass flow of Hg in CP #2.
The above values are based on one day.
a, Test value in the first day; b, Test value in the second day.

Table 7
Hg mass balance in the clinker to cement production process of CP #1.

Hg input/output	Material	Hg concentration ($\mu g \cdot kg^{-1}$)	Material input/output ($t \cdot d^{-1}$)	Hg input/output ($g \cdot d^{-1}$)	Hg percentage in input and output (%)
Hg input	Clinker	0.8 ± 0.3 (n = 3)	4241	3	2.1
	Particulate matter at the kiln head	16 ± 26 (n = 4)	96	1.5	0.9
	Fly ash from the coal-Fired power plants	36 ± 4 (n = 3)	424	15	9.4
	Gypsum	512 ± 15 (n = 3)	264	135	83.2
	Limestone	34 ± 22 (n = 3)	212	7	4.4
	Total			163	100
Hg output	Cement products	29 ± 1.4 (n = 6)	5237	152	100
Hg output/input percentage (%)		93			

from different raw materials and fueled coal (Table 5), and Hg stored in the raw meal was roughly steady with time elapse (Fig. 4). In contrast, only 15% of Hg input was ultimately discharged into atmosphere or as clinker in CP #2, with the remaining 85% trapped in the production system (Table 6).

To characterize the enrichment and cycling capacity of Hg in the rotary kiln, the pre-calcining + preheating cyclones and raw mill system, Hg enrichment factor was calculated according to Wang et al. (2016):

$$\text{Mercury Enrichment Factor} = \frac{\text{total mercury in the kiln system}}{\text{input mercury per day}} = \frac{(\text{mercury in raw meal} + \text{mercury in coal})}{(\text{mercury in raw and auxiliary materials} + \text{mercury in coal})} \quad (1)$$

The Hg enrichment factor was 5.9 and 104 for CP #1 and CP #2, respectively, suggesting that much more intensified enrichment of Hg in CP #2 than in CP #1. The Hg enrichment factor found in CP #1 was in the range of those found for two CPs (3.4–8.8) reported by Wang et al. (2016). The much higher value in CP #2 suggested that this CP, only with several month operation, was in accumulating stage for Hg, in contrast to the equilibrium stage as seen in CP #1 that operate 1.5 years. The particulate matter captured by APCDs at the kiln tail always contained much higher Hg concentration (1651–3029 μg kg^{-1}) than in various raw material (7–233 μg kg^{-1}), due to the adsorption of Hg from the flue gas in the raw mill. When these Hg-contained ashes are returned to the raw meal silo, Hg content in the raw meal will eventually increased. Thus, to reduce atmospheric Hg emissions, proper measures should be taken for the kiln tail ashes, such as breaking the Hg cycling and removing the kiln tail ashes from the production process.

During the clinker to cement production (Tables 7 and 8), gypsum accounted for most of Hg (89–94%) found in the cement, while clinker and other additional materials (such as fly ash and limestone) contributed to a total of less than 17% input. In the final cement products, Hg concentration varied with different brands, ranging from 28 to 30 μg kg^{-1} (N = 6) in CP #1 and from 14 to 29 μg kg^{-1} (N = 15) in CP #2. The cement-output weighted Hg content was estimated to be 29 μg kg^{-1} in CP #1 and 22 μg kg^{-1} in CP #2 (Tables 7 and 8), slightly lower than those (35–61 μg kg^{-1}) found in the other two CPs in China (Wang et al., 2014). The output/input ratio of Hg in the clinker to cement production ranged from 86 to 93% in the two studied CPs, indicating reliable calculation of Hg mass balance.

The material flow and Hg circulation in the whole production system of CP #1 and CP #2 are shown in Figs. 4 and 5. There is one internal and one external circulation of Hg in the clinker production process. The internal circulation refers to the circulation of Hg between raw mill and kiln system, and the external one refers to that between dust collector of kiln tail and the raw meal silo. A large amount of Hg is vaporized into the flue gas from raw meal when the rotary kiln and pre-calciner are at high temperatures (800–1450 °C). With the high temperature flue gas returning to cryogenic equipment (humidification tower and raw mill, 90–330 °C), most of the Hg in the flue gas is captured by particles and mixed with the raw materials, and re-entered into the pre-heater, pre-calciner and rotary kiln system and re-evaporate again.

Hg stored in the raw meal silo represented the main pool in the CPs, and was kept in a steady level (about 1842–1845 g d^{-1}) in CP #1. However, Hg in the raw meal silo of CP #2 increased every day, from 10,140 g d^{-1} on the first day to 10,223 g d^{-1} on the second day, with an accumulation rate of 83 g Hg·d^{-1}, suggesting that the production line was still in an enrichment state of Hg, which explains the low Hg emission levels in CP #2.

3.3. Mercury emission factors

Mercury emission factors (MEF) of the pre-calcined CPs were estimated from the total stack Hg emissions at the kiln tail and head (Tables 5 and 6). MEF from CP #1 was estimated to be 76.1 mg Hg·t^{-1} clinker, in which 31.4 mg Hg·t^{-1} clinker from the kiln head and 44.7 mg Hg·t^{-1} clinker from the kiln tail. The value would be reduced to 64.5 mg Hg·t^{-1} clinker if the contribution from the fueled coal was excluded. MEF from CP #2 was estimated to be 1.8 mg Hg·t^{-1} clinker (0.3 and 1.5 mg Hg·t^{-1} clinker from the kiln head and tail, respectively) (Tables 5 and 6). The non-coal emission in CP #2 was insignificant because the production line has not reached to a dynamic balance of Hg, thus its MEF excluded coal was not calculated here.

Compared with the Hg emission standards in USA for existing (55 lb Hg·Mt^{-1} clinker, equivalent to 25 mg Hg·t^{-1} clinker) and new CPs (21 lb Hg·Mt^{-1} clinker, equal to 9.5 mg Hg·t^{-1} clinker) (USEPA, 2011), the MEF from CP #1 exceeded their standards substantially, while that from CP #2 was within the standards (Table S1 and Fig. S3).

Existing studies showed that MEF ranged from 1.8 to 253 mg Hg·t^{-1} clinker and mostly below 80 mg Hg·t^{-1} clinker based on results of about 20 CPs worldwide (Table S1). The MEF (91–253 mg Hg·t^{-1} clinker) from four rotary kiln CPs in Hebei and Inner Mongolia in China (Miao et al., 2015) were obviously higher than the other CPs. The MEF of CP #1 in the present study is at the median range of the reported values worldwide, and is comparable to those measured by Wang et al. (2014) (62–72 mg Hg·t^{-1} clinker) and Zhang et al. (2016) (16–49 mg Hg·t^{-1} clinker). The MEF of CP #2 is the lowest among the reported values, even smaller than those of the two shaft kilns (3.3–3.6 mg Hg·t^{-1} cement) and two rotary kilns (9–12 mg Hg·t^{-1} cement) studied by Li (2011) (MEF based on cement is slightly lower than that based on clinker because cement is a mixture of clinker and a portion of additional materials). In addition, Renzoni et al. (2010) summarized 1681 emission measurement results in 62 countries, and concluded that the average Hg concentration in flue gas was 20 μg m^{-3} and the MEF was 35 mg Hg·t^{-1} clinker. Collectively, MEF in the pre-calcined CP is influenced by a range of factors, such as the Hg input, the raw mill operation conditions, and the methods for kiln tail ash treatment (Wang

Table 8
Hg mass balance in the clinker to cement production process of CP #2.

Hg input/output	Material	Hg concentration (μg·kg^{-1})	Material input/output (t·d^{-1})	Hg input/output (g·d^{-1})	Hg percentage in input and output (%)
Hg input	Clinker	1.2 ± 0.8 (n = 5)	5026	6	3.5
	Particulate matter at the kiln head	0.2 ± 0.1 (n = 5)	134	0.03	0.0
	Fly ash from the coal-Fired power plants	2 ± 1 (n = 5)	754	2	1.1
	Gypsum	521 ± 200 (n = 5)	302	157	94.4
	Limestone	6.5 ± 2.1 (n = 5)	251	2	1.0
	Total			167	100
Hg output	cement products	22 ± 4 (n = 15)	6467	143	100
Hg output/input percentage (%)		86			

et al., 2014; Renzoni et al., 2010).

The production of cement clinker in Guizhou Province in 2014 was 6.27×10^7 t (China cement magazine Co., Ltd, 2015). Using the average MEF (39.0 mg Hg·t^{-1} clinker) obtained at the two CPs discussed above, atmospheric Hg emission from the whole cement industry in Guizhou was estimated to be 2.44 t in 2014, similar to that estimated for 2012 (2.05 t) by Hua et al. (2016). The estimated value from the present study would account for 15.8% of the total anthropogenic Hg emissions in the province based on the 2014 value (15.44 t) given by Wu et al. (2016). It should be noted that field measurement data on Hg emissions are still very limited for the province, the other parts of China, and the rest of the world, and existing emission inventories are believed to have large uncertainties (Zhang et al., 2016).

4. Conclusions

Atmospheric Hg emissions are characterized for two CPs based on the measured Hg concentrations in flue gas and solid materials. Total Hg concentrations in the stack flue gas of two pre-calciner CPs are both lower than the national emission standard for flue gas of cement industry in China. Hg discharged from the stack at kiln tail accounts for most of the Hg output (50–58%), followed by that from the kiln head (11–41%), and negligible amount from the clinker. Due to the high Hg^p removal efficiencies in the two CPs, Hg is mainly emitted in the form of Hg^{2+}, followed by Hg^0, and with very low levels of Hg^p.

Analysis of Hg contents in solid samples of the clinker production process revealed raw materials as the main contributors (67.5–84.7%, limestone accounts for 41.4–56.4%) and fueled coal as a minor contributor (15.3–32.5%) to the total Hg input in the CPs. The Hg output/input ratio and enrichment factor indicated that Hg in CP #1 had reached to a dynamic balance, while that in CP #2 was still in an accumulation state. The Hg emission factors were estimated to be 76.1 and 1.8 mg Hg·t^{-1} clinker for CP #1 and CP #2, respectively, with the former exceeding the Cement kiln harmful air pollutant discharge standards. Results from the present study indicate that Hg emissions from CPs are complicated processes and more field studies are needed to reduce the uncertainties in Hg emission estimates for cement production in China.

Acknowledgements

This work is financially supported by K.C.Wong Education Foundation, the Environmental Science and Technology Project of Guizhou Environmental Protection Department (No. [2013]8) and the Natural Science Foundation of China (No. U1612442, 41373056). The authors greatly appreciate Xiaojun Chen and Xiaochun Liu for their hard work during the field sampling.

Appendix A. Supplementary data

Supplementary data to this article can be found online at https://doi.org/10.1016/j.atmosenv.2018.11.011.

References

Bureau of statistics of Guizhou Province, 2017. Guizhou Statistical Yearbook. China Statistics Press (In Chinese).
Chang, M.B., Wu, H.T., Huang, C.K., 2000. Evaluation on speciation and removal efficiencies of mercury from municipal solid waste incinerators in Taiwan. Sci. Total Environ. 246, 165–173.
China Cement Magazine Co, Ltd, 2015. China Cement Almanac. China Cement Almanac Press (In Chinese).
Galbreath, K.C., Zygarlicke, C.J., 2000. Mercury transformations in coal combustion flue gas. Fuel Process. Technol. 65–66, 289–310.
He, P., Zhang, X.B., Peng, X.L., Wu, J., Jiang, X.M., 2016. Effect of fly as composition on the retention of mercury in coal-combustion flue gas. Fuel Process. Technol. 142, 6–12.
Hua, S.B., Tian, H.Z., Wang, K., Zhu, C.Y., Gao, J.J., Ma, Y.L., Xue, Y.F., Wang, Y., Duan, S.H., Zhou, J.R., 2016. Atmospheric emission inventory of hazardous air pollutants from China's cement plants: temporal trends, spatial variation characteristics and scenario projections. Atmos. Environ. 128, 1–9.
Landis, M.S., Keeler, G.J., Al-Wali, K.I., Stevens, R.K., 2004. Divalent inorganic reactive gaseous mercury emissions from a mercury cell chlor-alkali plant and its impact on near-field atmospheric dry deposition. Atmos. Environ. 38, 613–622.
Lee, G., Kim, P., Han, Y., Holsen, T., Lee, S., 2014. Tracing sources of total gaseous mercury to Yongheung island off the coast of Korea. Atmosphere 5, 273–291.
Li, W.J., 2011. Characterization of Atmospheric Mercury Emissions from Coal-fired Power Plant and Cement Plant. Southwest University (In Chinese with English abstract).
Lindberg, S., Bullock, R., Ebinghaus, R., Engstrom, D., Feng, X.B., Fitzgerald, W., Pirrone, N., Prestbo, E., Seigneur, C., 2007. Panel on Source Attribution of Atmospheric Mercury. A synthesis of progress and uncertainties in attributing the sources of mercury in deposition. Ambio 36, 19–32.
Ma, B.G., 2007. New Dry Process Cement Production Process. Chemical Industry Press (In Chinese).
Miao, J., Zhang, C., Wang, X.F., Liu, Y., Zhang, F., Guo, L., Qian, F., 2015. Research of mercury emission characteristics from cement kilns. Environ. Pollut. Control. 37, 13–16 (In Chinese with English abstract).
Mlakar, T.L., Horvat, M., Vuk, T., Stergaršek, A., Kotnik, J., Tratnik, J., Fajon, V., 2010. Mercury species, mass flow and processes in a cement plant. Fuel 89, 1936–1945.
National Bureau of Statistic of China, 2017. China Statistical Yearbook. China Statistics Press (In Chinese).
Nriagu, J.O., 1989. A global assessment of natural sources of atmospheric trace metals. Nature 338, 47–49.
Nriagu, J.O., Pacyna, J.M., 1988. Quantitative assessment of worldwide contamination of air, water and soil by trace metals. Nature 333, 134–139.
Pacyna, E.G., Pacyna, J.M., 2002. Global emission of mercury from anthropogenic sources in 1995. Water Air Soil Pollut. 137, 149–165.
Pacyna, E.G., Pacyna, J.M., Steenhuisen, F., Wilson, S., 2006. Global anthropogenic mercury emission inventory for 2000. Atmos. Environ. 40, 4048–4063.
Pacyna, E.G., Pacyna, J.M., Sundseth, K., Munthe, J., Kindbom, K., Wilson, S., Steenhuisen, F., Maxson, P., 2010. Global emission of mercury to the atmosphere from anthropogenic sources in 2005 and projections to 2020. Atmos. Environ. 44, 2487–2499.
Pham, T., Junpen, A., Garivait, S., 2015. An investigation of atmospheric mercury from power sector in Thailand. Atmosphere 6, 490–502.
Pirrone, N., Cinnirella, S., Feng, X.B., Finkelman, R.B., Friedli, H.R., Leaner, J., Mason, R., Mukherjee, A.B., Stracher, G.,B., Streets, D.G., Telmer, K., 2010. Global mercury emissions to the atmosphere from anthropogenic and natural sources. Atmos. Chem. Phys. 10, 5951–5964.
Renzoni, A., Zino, F., Franchi, E., 1998. Mercury levels along the food chain and risk for exposed populations. Environ. Res. 77, 68–72.
Renzoni, R., Ullrich, C., Belboom, S., Germain, A., 2010. Mercury in the Cement Industry. Report of CEMBUREAU-CSI.
Schroeder, W.H., Munthe, J., 1998. Atmospheric mercury-An overview. Atmos. Environ. 32, 809–822.
Senior, C., Montgomery, C.J., Sarofim, A., 2010. Model for behavior of mercury in Portland cement kilns. Ind. Eng. Chem. Res. 49, 1436–1443.
Sheu, G.R., Mason, R.P., 2001. An examination of methods for the measurements of reactive gaseous mercury in the atmosphere. Environ. Sci. Technol. 35, 1209–1216.
Sikkema, J.K., Alleman, J.E., Ong, S.K., Wheelock, T.D., 2011. Mercury regulation, fate, transport, transformation, and abatement within cement manufacturing facilities: Review. Sci. Total Environ. 409, 4167–4178.
Streets, D.G., Devane, M.K., Lu, Z., Bond, T.C., Sunderland, E.M., Jacob, D.J., 2011. All-time releases of mercury to the atmosphere from human activities. Environ. Sci. Technol. 45, 10485–10491.
Streets, D.G., Horowitz, H.M., Jacob, D.J., Lu, Z.F., Levin, L., Schure, A.F.H., Sunderland, E.M., 2017. Total mercury released to the environment by human activities. Environ. Sci. Technol. 51, 5969–5977.
Tang, X.Y., 2004. Trace Elements in Chinese Coal. The Commercial Press (In Chinese).
Tian, H.Z., Wang, Y., Xue, Z.G., Cheng, K., Qu, Y.P., Chai, F.H., Hao, J.M., 2010. Trend and characteristics of atmospheric emissions of Hg, As, and Se from coal combustion in China, 1980-2007. Atmos. Chem. Phys. 10, 11905–11919.
Travnikov, O., 2005. Contribution of the intercontinental atmospheric transport to mercury pollution in the Northern Hemisphere. Atmos. Environ. 39, 7541–7548.
UNEP, 2002. Global Mercury Assessment. Geneva, Switzerland.
UNEP, 2013. Global Mercury Assessment 2013: Sources, Emissions, Releases and Environmental Transport. UNEP Chemicals Branch, Geneva, Switzerland.
USEPA, 2011. National emission standards for hazardous air pollutants from the portland cement manufacturing industry and standards of performance for Portland cement plants. Fed. Regist. 63 EPA 40 CFR Parts 60.
Wang, F.Y., Wang, S.X., Zhang, L., Yang, H., Wu, Q., Hao, J.M., 2014. Mercury enrichment and its effects on atmospheric emissions in cement plants of China. Atmos. Environ. 92, 421–428.
Wang, F.Y., Wang, S.X., Zhang, L., Yang, H., Wu, Q., Hao, J.M., 2016. Characteristics of mercury cycling in the cement production process. J. Hazard Mater. 302, 27–35.
Wang, X.L., 2017. Research on the Characteristics of Mercury Emission and the Potention of Emission Reduction in the Process of Cement Production. Zhejiang University (In Chinese with English abstract).
Wang, Y.M., Su, M.J., Zhang, L., 2007. Classification of sulphoaluminate cement and the difference between its varieties. China Cem 2, 32–36 (In Chinese with English abstract).
Won, J.H., Lee, T.G., 2012. Estimation of total annual emissions from cement manufacturing facilities in Korea. Atmos. Environ. 62, 265–271.
World Health Organization (WHO), 1991. Environmental Health criteria. In: Inorganic Mercury. vol. 118 World Health Organization, Geneva.

Wu, C.Z., 1999. Suggestions on the classification of general cements of China. Bull. Chin. Ceram. Soc. 5, 59–62 (In Chinese with English abstract).
Wu, Q.R., Wang, S.X., Li, G.L., Liang, S., Lin, C.J., Wang, Y.F., Cai, S.Y., Liu, K.Y., Hao, J.M., 2016. Temporal trend and spatial distribution of speciated atmospheric mercury emissions in China during 1978-2014. Environ. Sci. Technol. 50, 13428–13435.
Wu, Y., Wang, S., Streets, D.G., Hao, J.M., Chan, M., Jiang, J.K., 2006. Trends in anthropogenic mercury emissions in China from 1995 to 2003. Environ. Sci. Technol. 40, 5312–5318.
Xiao, Z.M., Li, J.L., 2006. Cement Technology. Chemical Industry Press (In Chinese).
Yang, H., 2014. Study on Atmospheric Mercury Emission and Control Strategies from Cement Production in China. Tsinghua University (In Chinese with English abstract).
Zhang, C., Zhang, Y.H., Wand, Y.M., Wang, D.Y., Luo, C.Z., Xu, F., He, X.Q., 2017. Characteristics of mercury emissions from modern dry processing cement plants in Chongqing. Environ. Sci. 6, 2287–2293 (In Chinese with English abstract).
Zhang, L., 2007. Research on Mercury Emission Measurement and Estimate from Combustion Resources. Zhejiang University (In Chinese with English abstract).
Zhang, L., Wang, S., Wang, L., Wu, Y., Duan, L., Wu, Q., Wang, F., Yang, M., Yang, H., Hao, J., Liu, X., 2015. Updated emission inventories for speciated atmospheric mercury from anthropogenic sources in China. Environ. Sci. Technol. 49 (5), 3185–3194.
Zhang, L., Wang, S.X., Wu, Q.R., Wang, F.Y., Lin, C.J., Zhang, L.M., Hui, M.L., Hao, J.M., 2016. Mercury transformation and speciation in flue gases from anthropogenic emission sources: a critical review. Atmos. Chem. Phys. 16, 2417–2433.
Zhang, Y., Jaeglé, L., 2013. Decreases in mercury wet deposition over the United States during 2004–2010: roles of domestic and global background emission reductions. Atmosphere 4, 113–131.
Zhou, G.Z., Peng, B.L., 2005. Introduction to the Cement Production Process. Wuhan University of Technology Press (In Chinese).